

High levels of alkali-metal storage in thin films of hexa-*peri*-hexabenzocoronene

M. Keil^{a)}

Department of Physics, IFM, Linköping University, S-581 83 Linköping, Sweden

P. Samorí

Department of Physics, Humboldt University Berlin, Invalidenstrasse 110, D-10115 Berlin, Germany

D. A. dos Santos

Université de Mons-Hainaut, Place du Parc 20, B-7000 Mons, Belgium

J. Birgerson and R. Friedlein^{b)}

Department of Physics, IFM, Linköping University, S-581 83 Linköping, Sweden

A. Dkhissi

Université de Mons-Hainaut, Place du Parc 20, B-7000 Mons, Belgium

M. Watson and K. Müllen

Max-Planck-Institut for Polymer Research, Ackermannweg 10, D-55128 Mainz, Germany

J. L. Brédas

Université de Mons-Hainaut, Place du Parc 20, B-7000 Mons, Belgium and Department of Chemistry, University of Arizona, Tucson, Arizona 85721

J. P. Rabe

Department of Physics, Humboldt University Berlin, Invalidenstrasse 110, D-10115 Berlin, Germany

W. R. Salaneck

Department of Physics, IFM, Linköping University, S-581 83 Linköping, Sweden

(Received 28 August 2001; accepted 27 March 2002)

The affects of alkali-metal atoms on the electronic structure of disordered and highly ordered thin films of the medium-size aromatic hydrocarbon hexa-*peri*-hexabenzocoronene (HBC) have been investigated by valence and core level photoelectron spectroscopies—ultraviolet photoelectron spectroscopy (UPS) and x-ray photoelectron spectroscopy (XPS)—and accompanying quantum-chemical calculations. Deposition of Li or Na atoms *in situ* leads to new spectral features in the UPS spectra, which are related to formerly unoccupied molecular states. The binding energies and intensities of these features depend on the nature of the counterion. The smaller Li ion exhibits a stronger influence on the electronic structure than its sodium counterpart. In the intercalation of sodium into ordered films, a high degree of molecular order is preserved, and, at high deposition levels, a surface dipole is formed that is associated with the layered structure of the compound. Remarkably, high levels of alkali-metal storage of at least one alkali-metal atom for each four carbon atoms have been observed, indicating clearly the potential use of these graphene materials in lithium-ion batteries with a high charge-storage capacity. © 2002 American Institute of Physics. [DOI: 10.1063/1.1479717]

INTRODUCTION

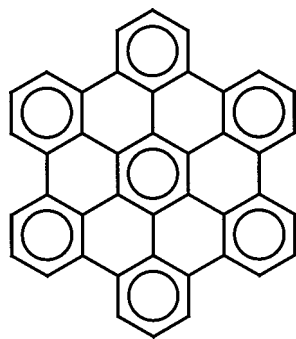
The development of new materials for high-density energy storage represents one of the major challenges to the scientific community.¹ Rechargeable batteries, in particular “lithium-ion” batteries, are one of the most important commercialized energy storage devices. The most common structure of lithium-ion batteries involves a lithium metal oxide (e.g., LiCoO₂) cathode, a lithium-conducting electrolyte, and a carbonaceous anode. One limiting factor for the performance of this type of device is the specific charge capacity of

the electrodes. For graphite at ambient pressure, this is about 372 mA h/g, as obtained in the first stage lithium intercalation compound (GIC) LiC₆.¹ To overcome this limit, a great deal of effort has been devoted to finding alternative electrode materials. In this context, it has been shown recently that high levels of lithium content, LiC_{2.67}, can be attained in either highly oriented pyrolytic graphite (HOPG) at high pressure² or, up to a limit of LiC₂, in highly disordered carbonaceous materials prepared from heat treatment of polymers such as poly-*para*-phenylene.³

Large- and medium-size polycyclic aromatic hydrocarbons (PAH's) represent a new class of synthetic materials with promising electronic properties.^{4,5} A novel synthetic strategy allows the design of planar graphenelike nano-

^{a)}Present address: Obducat A.B., S-201 25 Malmö, Sweden.

^{b)}Author to whom correspondence should be addressed. Electronic mail: raifr@ifm.liu.se



Scheme 1. Chemical formula of hexa-*peri*-hexabenzocoronene.

objects with different sizes and functionalities in the peripheral positions.⁶ These molecules represent model systems that can provide new insights into the mechanism of alkali-metal storage in carbon-based materials. In addition, for applications in molecular electronics, particularly for the development of molecular nanowires,^{5,7,8} it is of prime importance to increase the conductivities of molecular solid films. Potential charge carriers might be created by oxidizing or reducing the π -conjugated molecules, by forming charge transfer salts.⁹ For the generation of *n*- or *p*-type charge carriers, the term “doping” has been used, in analogy to inorganic semiconductors,¹⁰ although, since the origin and mechanisms are different, perhaps other terminology may be more appropriate. The reduction of π -conjugated molecules in thin solid films may easily be achieved by the addition of alkali-metal atoms.⁹ In this context, finding suitable dopant species (or, “intercalation” species, if one so chooses) is an essential step towards the control of the electronic properties of the chosen molecular system.

Here, we report the results of a study of the doping of molecular solid films of the medium-sized aromatic hydrocarbon hexa-*peri*-hexabenzocoronene (HBC, $C_{42}H_{18}$), using lithium or sodium atoms. In order to understand the influence of structural order in the doped film on electronic properties, samples with a different degree of molecular order have been investigated. The HBC molecule, as sketched in Scheme 1, can be viewed as a well-defined segment of a graphene sheet. The D_{6h} symmetry results in a number of degenerate electronic states. Most notably, the highest occupied (HOMO) and lowest unoccupied (LUMO) molecular orbitals are both doubly degenerate. The evolution of the valence band electronic structure as a function of the addition of Li and Na atoms to thin solid films, monitored by x-ray photoelectron spectroscopy (XPS), has been studied by ultraviolet photoelectron spectroscopy (UPS). To aid in the interpretation of the experimental data, quantum-chemical calculations on the charged molecule, without the counterions, were performed.

EXPERIMENTAL PROCEDURES

HBC films with a nominal thickness of 20 nm were prepared by vapor deposition in ultra high vacuum (UHV) at a base pressure of 5×10^{-10} mbar onto various substrates, chosen specifically to provide films with a high or low degree of molecular order. The film thickness was monitored using a quartz microbalance. As described elsewhere,⁷ a deposition at a rate of about 3 Å/min onto freshly cleaved, highly ori-

ented pyrolytic graphite (HOPG) (ZYB quality, Union Carbide Corp.) results in epitaxially ordered, polycrystalline films formed in a layer-by-layer growth, with the molecular planes oriented parallel to the [0001] surface of the substrate. The lateral dimensions of these molecular crystals are on the micrometer scale. Evidence for strong intermolecular interactions due to π - π stacking of the HBC molecules aligned parallel to each other has been found with UPS. On the other hand, highly disordered films are obtained by deposition onto oxidized Si wafers, or polycrystalline Au films. Here, the HBC films are made up of grains with diameters between 25 and 30 nm. X-ray absorption spectroscopy and atomic force microscopy did not indicate any significant degree of lateral order or azimuthal orientation of the adsorbed molecules. Sodium was deposited on either the epitaxially ordered or highly disordered molecular films. However, since the Li(1s) binding energy is near that of the Au(5p) level, lithium atoms were deposited on disordered films grown on oxidized Si wafers as substrates.

Deposition of Li- or Na-atoms was carried out in a separate preparation chamber of the photoelectron spectrometer by a stepwise increasing deposition from standard SAES® alkali getter sources that were carefully degassed prior to the experiments. During the vapor deposition steps, the chamber pressure was always less than 2×10^{-9} mbar. However, the sample resided inside a copper cylinder held at less than 20 K, wherein the total pressure is near 1×10^{-10} mbar, as determined in separate experiments. This environment assures minimal oxidation during the alkali-metal deposition. On the other hand, the substrates were held at room temperature during deposition of the metal atoms. Eventually, to obtain indications of thermodynamic stability, samples were annealed at up to 550 K for 10 min.

UPS and XPS measurements were performed in an electron spectrometer designed and constructed in Linköping. UPS was carried out with monochromatized He I (21.22 eV) radiation, with an applied sample bias of 50 V. Spectra of standard (e.g., gold) substrates are well reproduced with the 50 V bias, but real angle-dependent UPS is somewhat compromised. The ionization potentials of both pristine and doped samples were obtained through the energy of the cut-off of the secondary electron spectrum, as discussed elsewhere.¹¹ The net energy resolution during UPS was about 0.2 eV, as determined from the 90%-to-10% intensity points of the Fermi edge of a clean gold substrate. All spectra were recorded under identical conditions (sample position, light intensity, electron-energy-analyzer settings and other recording parameters), and plotted on an energy scale relative to the vacuum level. After each step of deposition of the alkali metals, the nominal stoichiometry was determined by XPS from the intensity of the C, O, and Li or Na(1s) core-level lines. The energy resolution for XPS was about 1.4 eV and 0.7 eV, for nonmonochromatized Al($K\alpha$) and Mg($K\alpha$), respectively, as determined from the width of the Au(4f) substrate core-level lines. After subtraction of the Shirley background, as motivated elsewhere,¹² the individual spectra, including both main structures and shakeup satellites, were integrated. Finally, each value was divided by the particular sensitivity factor based on the photoelectric cross sections

for Mg($K\alpha$) or Al($K\alpha$) radiation.¹³ The experimentally determined transmission function of this electron energy analysis system is flat over the energy regions of interest, and thus corrections for transmission are not necessary. Given the rather low-energy resolution of the XPS data, no attempt was made to discuss the lines shapes or even the binding energy or of the core-level lines. XPS data were used only to monitor the amount of each element in the samples. On the other hand, no distinguished fine structure or sudden binding energy changes were detected during metal atom deposition that could have indicated the formation of stoichiometric phases of the compounds.¹⁴

QUANTUM-CHEMICAL CALCULATIONS

The geometric and electronic structure of pristine or reduced HBC molecules was modeled as follows. The geometric parameters were determined using the semiempirical Austin model 1 (AM1) Hamiltonian.¹⁵ Then the optimized geometry was used as input to the electronic structure calculations carried out using the valence effective Hamiltonian (VEH) method.^{16,17} In order to compare the calculated results with the UPS spectra, the energy spectrum of the molecular eigenvalues was convoluted with Gaussian functions with a full width at half maximum (FWHM) of 0.7 eV, as used previously.⁷ Since Hartree–Fock-based methods are known to provide valence electronic structures which are too wide in energy, the simulated density of valence states (DOVS) was contracted by a factor of 1.1 eV (see discussion in Ref. 7). Finally, the spectra were rigidly shifted to lower binding energies to account for solid-state polarizations effects.¹⁸

RESULTS AND DISCUSSIONS

The UPS spectra of ordered and disordered pristine HBC films have been described previously⁷ (see also the section titled Experimental Procedures, above). The spectrum for the disordered films is replotted here for reference in Fig. 1(a). It exhibits two strong π -derived features: the peak at 5.8 eV (labeled 1) represents three electronic π states, and the peak at 7.1 eV (labeled 2) represents six π states. Generally, the deposition of alkali-metal atoms leads to the appearance of new features in the low-binding-energy portion of the spectrum, indicating charge transfer from the Li or Na atoms to the HBC molecules.

First, films with a low degree of molecular order are discussed. Figure 1, panels (b) to (g), displays the evolution of the spectra with increasing Na deposition. For low deposition levels, a single peak (labeled 1*) with a tail on the low-binding-energy side appears at about 4.1 eV. For larger doping levels, this tail develops into a strong second peak at 3.1 eV (marked as 2*). The formation of the new structures is accompanied by a reduction of the work function from 4.0 ± 0.1 eV to 2.1 ± 0.1 eV. No spectral weight is observed in the vicinity of the Fermi level, at any doping level. Furthermore, for levels of up to about 8.9 ± 0.5 Na atoms per molecule, the amount of oxygen, which is a sensitive indication of an oxide layer at the surface, did not increase, and stayed well below 2% of the number of C atoms. This demonstrates the following:

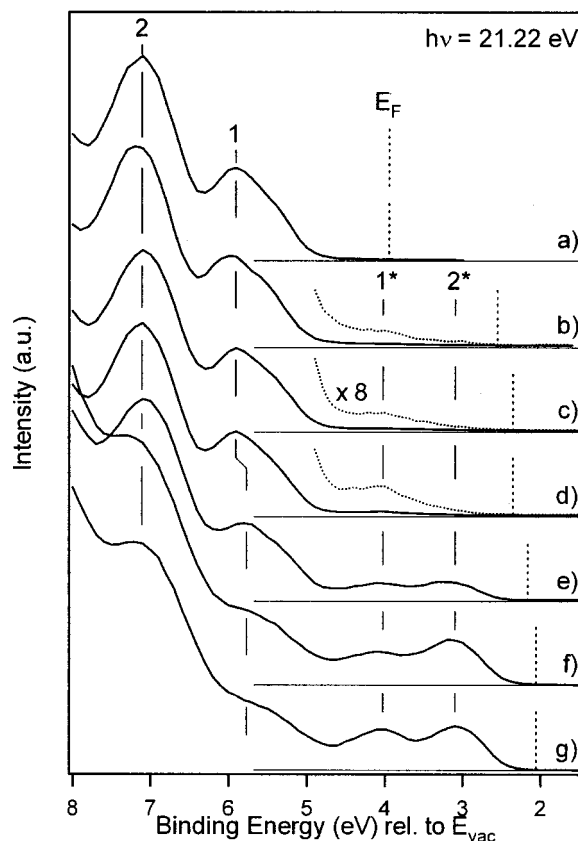


FIG. 1. Evolution of the π region of He I UPS spectra of a 20 nm thick HBC film supported on polycrystalline Au as a function of increasing Na deposition. Dotted curves correspond to intensities multiplied by a factor of 8. The following Na per molecule ratios and work functions are observed: (a) pristine, $\phi=4$ eV; (b) 0.6 Na/molecule, $\phi=2.6$ eV; (c) 1.1 Na/molecule, $\phi=2.4$ eV; (d) 1.6 Na/molecule, $\phi=2.4$ eV; (e) 6 Na/molecule, $\phi=2.2$ eV; (f) 8.9 Na/molecule, $\phi=2.1$ eV; (g) 13 Na/molecule, $\phi=2.1$ eV.

(a) the atoms penetrate into the film, such that the surface is not covered by a metallic alkali film, and

(b) the film remains semiconducting (but this does not negate an increase in conductivity).

To explore the origin of the new spectral features, the results of quantum-chemical calculations of the pristine and reduced states of the HBC molecule are used. The results, plotted in Figs. 2 and 3, indicate that the additional electrons lead to a geometrical deformation of the molecule in the reduced state as compared to the ground state. This leads to a lifting of the degeneracy of electronic levels, an effect commonly known as the Jahn–Teller effect. Above a level of about 10 electrons per molecule, however, an instability of the molecular structure, characterized by a breakage of the molecular bonds, appears. These theoretical results are consistent with the experimental spectra, especially indicating the formation of two charge-transfer-induced structures. In agreement with the experimental observations, only one peak appears at low doping levels. In the theoretical results, upon addition of more than 8 electrons, this peak is accompanied by a second one at lower binding energies. The remarkable agreement between experiment and theory appears to confirm the validity of a simple picture corresponding to the filling of unoccupied molecular orbitals with the additional electrons: peak 1* arises from filling of both the doubly de-

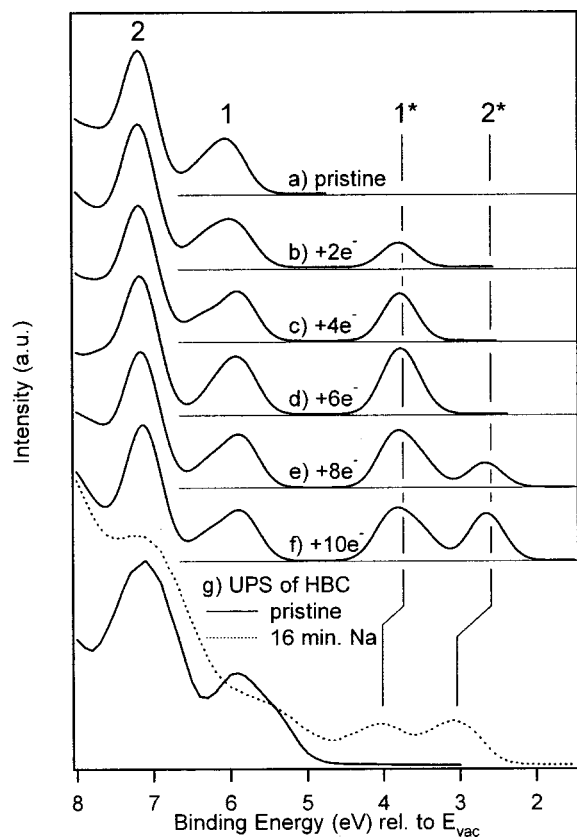


FIG. 2. VEH-simulated spectra of HBC and its reduced states HBC^{2-} , HBC^{4-} , HBC^{6-} , HBC^{8-} and HBC^{10-} . Panel (g) allows the comparison with the UPS spectra of pristine HBC film [Fig. 1(a)] and HBC plus 13 ± 0.5 Na atoms/molecule [Fig. 1(g)].

generate original LUMO, and one additional orbital at lower binding energy; these are separated by only 0.2 eV. The appearance of just one new peak 1^* in the $(\text{HBC})^{-6}$ spectrum of Fig. 2(d) has its origin in the Gaussian function convolution of the three eigenvalues. A charge population analysis of the sextuply charged molecule $(\text{HBC})^{-6}$ indicates the spatial distribution of the additional electrons as plotted in Fig. 3.

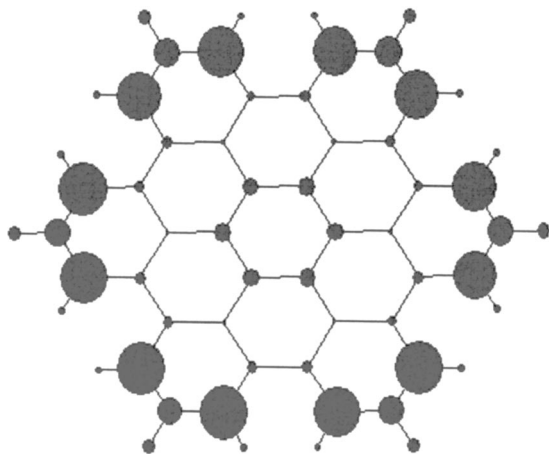


FIG. 3. AM1-calculated spatial distribution of the six additional electrons of the HBC^{6-} reduced state. Each of the biggest 12 circles symbolizes -0.41 extra charges. This leads to a total extra charge of 4.9 electrons at these 12 periphery positions. The remaining 1.1 electrons are spread out over the rest of the molecule.

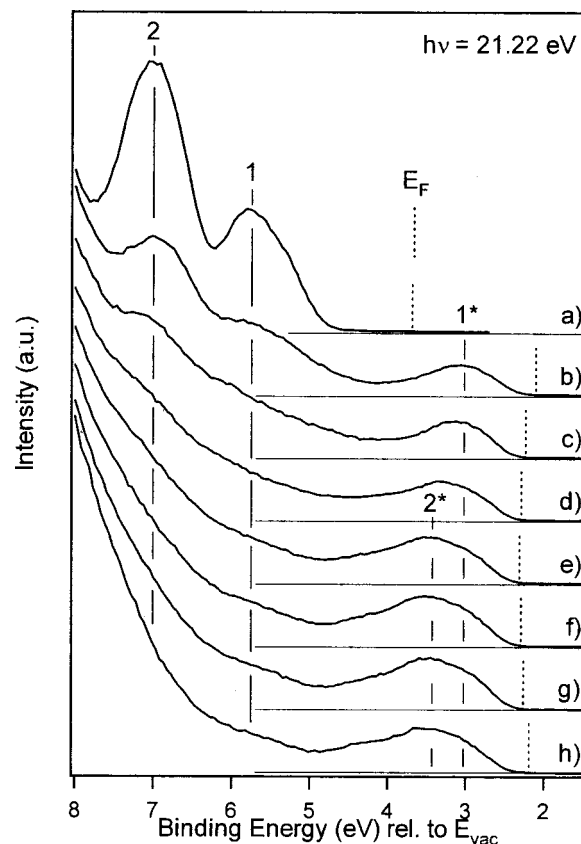


FIG. 4. Evolution of the π region of the He I UPS spectra of a 20 nm thick HBC film adsorbed on oxidized Si as a function of increasing Li deposition. The following Li per molecule ratios and work functions are observed: (a) pristine, $\phi=3.7$ eV; (b) 1.7 Li/molecule, $\phi=2.1$ eV; (c) 3.0 Li/molecule, $\phi=2.3$ eV; (d) 5.4 Li/molecule, $\phi=2.3$ eV; (e) 6.9 Li/molecule, $\phi=2.4$ eV; (f) 10.3 Li/molecule, $\phi=2.3$ eV; (g) 10.9 Li/molecule, $\phi=2.3$ eV; (h) 12.6 Li/molecule, $\phi=2.2$ eV.

The excess charge is stored on the periphery of the molecule. This charged molecule is also highly symmetric (D_{6h}), with uniform bond lengths in the innermost ring of the molecule. Adding more than six electrons requires the filling of additional orbitals, which results in the appearance of peak 2^* in the spectra of Fig. 2, panels (e) and (f). These orbitals are separated from the first group by between 1 and 1.8 eV. As shown by the comparison with the experimental curves in Fig. 2(g), the absolute binding energies of the two doping-induced peaks (labeled 1^* and 2^*) are, however, not perfectly reproduced in the theoretical results. The main reasons for disagreement are related to the fact that the calculations do not include explicitly the nature of the counterions and electron correlation effects.^{19,20}

To address the influence of the nature of the counterions, a series of doping experiments were performed on HBC films by varying the counterion. Films with a low degree of molecular order have been doped with smaller Li atoms instead of Na atoms. The UPS valence band spectra are shown in Fig. 4. The differences, with respect with the Na case, are striking. Instead of the well-separated two peaks only a single but broad structure appears, initially at 3.1 eV binding energy (labeled 1^*). This peak eventually grows in intensity with increasing doping. After additional deposition of Li atoms, the peak energy maximum is shifted to about 3.5 eV

(labeled 2*). Compared to the Na experiments, the order of appearance of the new structure in the spectra seems to be reversed: at low deposition levels, the additional structure arises predominantly on the low-binding-energy side of the spectra, near the Fermi level, and results in the appearance of peak 1*, whereas for higher levels, new structure grows mainly in the region between peaks 1 and 1*. Moreover, in contrast to the Na case, in the Li case the shift of the Fermi level takes place more suddenly, already at very low Li concentration, and then remains almost unchanged up to the highest levels. Small differences in the measured value of the Fermi level, as observed in Figs. 4(b) to 4(f), are within the resolution, about 0.2 eV, in the determination of the work function. Lithium ions are expected to interact somewhat differently with the molecules than sodium ions.²¹ Because of the smaller ionic radius, the positive charges on the Li-metal ions are located closer to the HBC molecules and can polarize the molecules more strongly. The presence of the lithium ions should then result in a stronger localization of electrons on specific parts of the molecule,²² which can lead to a further stabilization of specific orbitals. Furthermore, the lithium atom in such charge-transfer salts is close to the covalent bonding regime^{23–25} and might therefore have a greater influence on the electronic structure of the molecules, as compared to sodium.

Additional experiments were carried out on ordered HBC films grown on HOPG [0001]. For this type of sample, the Na/C ratio cannot be precisely determined using XPS because of the presence of an unknown amount of intensity in the C(1s) signal from the HOPG substrate. Instead, for an estimation (better than an order of magnitude), the Na concentration, as given in the caption of Fig. 5, was estimated from the intensity of the Na(1s) line by comparison with that of the HBC film, prepared on a gold substrate under otherwise identical conditions. The UPS spectra are shown in Fig. 5, as a function of increasing deposition of Na atoms. Again, as in the case of less ordered films, two new peaks appear. Generally, the spectra are very similar to those of less ordered films, which is consistent with the minor influence of the Na ions on the spatial electron density distribution within the molecules. However, two main differences are observed. First, the two new features (labeled 1* and 2*) appear together already at very low deposition levels. Second, the whole spectrum shifts to lower binding energies for higher doping levels. Remarkably, except at very low doping levels, this shift seems to be linear with the amount of sodium deposited.

The uniform decrease in binding energy of all the spectral features, by about 0.8 eV, between low and high intercalation levels, while the overall shape of the valence band spectrum is retained, is caused by a doping-level-dependent acceleration of the escaping photoelectrons in the surface region as a result of the formation of a surface dipole layer. The existence of such a dipole layer is related to the molecular order in the films, since it is not observed for the disordered films. It is known that the HBC molecules are oriented with the molecular planes parallel to the surface in films with thickness up to at least 10 nm.⁷ It seems that this dipole layer appears because of the layered structure of the film, which

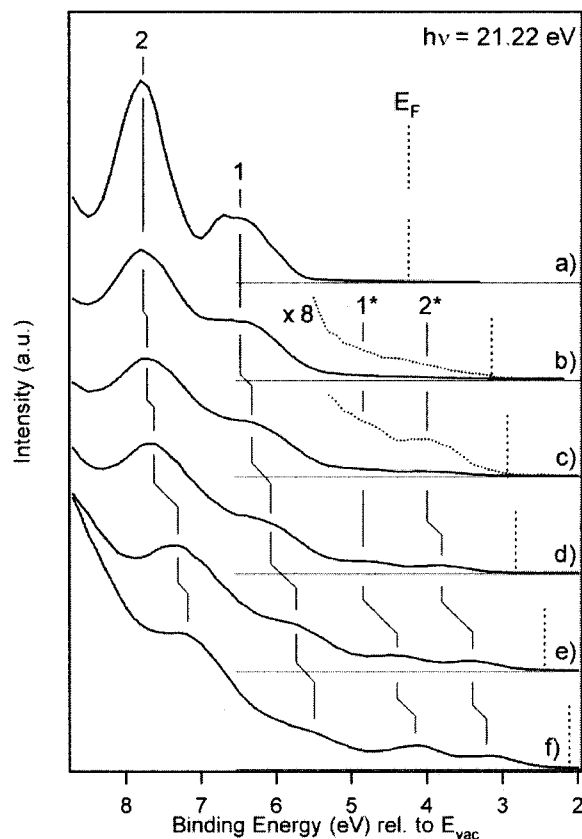


FIG. 5. Evolution of the π region of the He I UPS spectra of a 20 nm thick HBC film supported on HOPG as a function of increasing Na deposition. The dotted curves denote intensities that are multiplied by a factor of 8. The estimated Na-per-molecule ratios and work functions are (a) pristine, $\phi=4.3$ eV; (b) 0.6 Na/molecule, $\phi=3.2$ eV; (c) 1.9 Na/molecule, $\phi=3$ eV; (d) 3.9 Na/molecule, $\phi=2.9$ eV; (e) 6.2 Na/molecule, $\phi=2.5$ eV; (f) 11.6 Na/molecule, $\phi=2.2$ eV.

might be thought of as arising from an exclusive surface termination by alkali-metal ions (but possibly even involving several layers below the surface). This surface dipole layer may be a result of a slight tendency for surface segregation of a small amount of sodium atoms (ions) in ordered films, whereas in disordered films, a more homogeneous distribution of the alkali-metal atoms should occur.

The amount of surface oxygen contamination, from the residual gases, is another indication for the presence of alkali-metal atoms at the surface. In the ordered films, at moderate Na concentrations, the O/Na ratio is about 0.2. That is, the amount of oxygen increases with increasing deposition levels. On the other hand, for similar doping levels the disordered films remain almost unaffected by oxidation. These results are in agreement with an exclusive surface termination by alkali-metal ions in the molecularly ordered films. These results also argue against any possible buildup of charge at the film-substrate interface as a possible explanation of the binding energy shift observed for ordered films. Note that a more quantitative investigation of the ion-diffusion process using angle-resolved XPS, to determine the Na/C ratio as a function of angle of the emitted electrons, is not possible because of the contribution of the HOPG substrate to the intensity of the C(1s) signal. The presence of a surface dipole is further supported by the observation of the

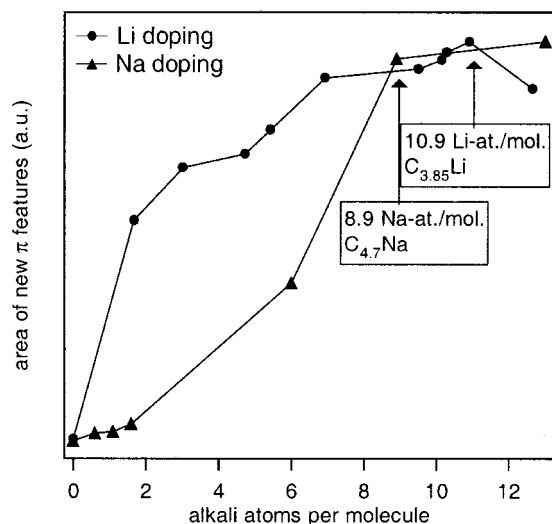


FIG. 6. Area under the curve of new features in the UPS spectra for increasing Li deposition onto a 20 nm thick HBC film adsorbed on oxidized Si (filled circles) and for increasing Na deposition onto a 20 nm thick HBC film adsorbed on polycrystalline Au (filled triangles) as a function of the number of alkali-metal atoms per molecule.

appearance of two new peaks already at low deposition levels, features 1* and 2* in Fig. 4. This splitting occurs because of the simultaneous occupation of several orbitals in the outermost layers of the film that are preferentially accessed in surface-sensitive spectroscopies. It is worth pointing out that this effect is different from an initial-state chemical shift caused by charge transfer (as measured relative to the Fermi level), which was recently observed on submonolayers of K atoms adsorbed on graphite.²⁶ The above observations implicitly indicate the survival of molecular order in the HBC films (on HOPG) upon doping. On the other hand, in contrast to the behavior of less-ordered HBC films, annealing of the ordered samples at 550 K does not result in a dedoping of the films. Therefore it is suggested that for crystalline HBC material, as for various C_{60} intercalation compounds,¹⁴ alkali-metal-atom doping results in the formation of thermodynamically stable phases with ordered architectures.

The maximum doping level that can be achieved in solid films of HBC was addressed by studying the saturation behavior of the doping-induced valence band features 1* and 2*. The integrated intensities (area under the curves) of these features are then proportional to the density of the newly occupied density of states (DOS) weighted by the photoelectric cross sections. The evolution of this area with increasing alkali-metal deposition is shown in Fig. 6. For Li-doped disordered HBC films, saturation is achieved at a doping level of about 10.9 ± 0.5 Li atoms per molecule, which corresponds to a C/Li ratio of 3.85 ± 0.2 . This level ($LiC_{3.85}$) is significantly higher than that reported to be obtained under ambient pressure for the stage-1 graphite intercalation compound LiC_6 .²⁷ For the Na-doped disordered HBC films, the saturation level is between 8.9 ± 0.5 and 13 ± 0.5 atoms per molecule, which corresponds to C/Na ratios of about 4 ± 0.7 . In this case (Na doping), almost no oxygen contamination could be observed, up to a level of about 6 Na atoms per

molecule, after which oxidation increases somewhat, but the O/C is still less than 0.04 at a level of 8.9 ± 0.5 Na atoms per molecule. Note also that, for the ordered films, the O/C ratio increases linearly with doping level, from almost zero in a pristine sample to about 0.02 at the highest doping level.

It is clear from this work that very similar high levels of doping of thin films of HBC molecules in UHV are achieved with either Li or Na atoms. Note that such high levels of alkali metal atom storage have been observed recently in other polycyclic aromatic hydrocarbons, for example, in perylene.²⁸

CONCLUSION

In the framework of the development of competitive energy storage systems based on environmentally friendly elements, future applications of carbon-based molecular materials for use as new types of electrodes can be foreseen. It is shown here that high levels of Li and Na storage in films of the aromatic hydrocarbon hexa-*peri*-hexabenzocoronene can be achieved. The combined results of photoelectron spectroscopy and quantum-chemical calculations reveal that the *n*-doping depends on both the type of alkali-metal atom employed and on the molecular order of the film. The smaller Li ion is found to have a stronger influence on the electronic structure than Na ions. In the alkali-metal doping of ordered films, molecular order is likely to be preserved, which corresponds to the formation of thermodynamically stable phases. However, near room temperature, the Na intercalation of the ordered film is less efficient than that for disordered films. Importantly, these present results indicate that batteries based upon HBC molecules may be fabricated with a charge storage capacity higher than that in currently available lithium-ion batteries based upon conventional graphite anodes.

ACKNOWLEDGMENTS

This work was carried out within the EU-TMR Project SISITOMAS (Project No. 0261). Research on condensed molecular solids and polymers in Linköping is supported in general by grants from the Swedish Science Research Council (V.R.), and the Swedish Foundation for Strategic Research (S.S.F.). The Linköping–Mons collaboration is supported by the European Commission through the EU-RTN project LAMINATE (HPRN-CT-2000-00135). The work in Mons is partly supported by the Belgium Federal Government “Inter-University Attraction Pole on Supramolecular Chemistry and Catalyses (PAI 4/11)” and FNRS-FRFC. The work at Arizona is partly supported by the National Science Foundation Grant No. (CHE-0071889).

¹G. Pistoia, *Lithium Batteries* (Elsevier, Amsterdam, 1994).

²V. A. Nalimova, D. Guerard, M. Lelaurain, and O. V. Fateev, *Carbon* **33**, 177 (1995).

³K. Sato, M. Noguchi, A. Demachi, N. Oki, and M. Endo, *Science* **264**, 556 (1994).

⁴A. Stabel, P. Herwig, K. Müllen, and J. P. Rabe, *Angew. Chem. Int. Ed. Engl.* **34**, 1609 (1995).

⁵A. M. v. d. Craats, J. M. Warman, K. Müllen, Y. Geerts, and J. D. Brand, *Adv. Mater.* **10**, 36 (1998).

⁶M. Müller, C. Kübel, and K. Müllen, *Chem.-Eur. J.* **4**, 2099 (1998).

- ⁷M. Keil, P. Samorí, D. A. dos Santos *et al.*, *J. Phys. Chem. B* **104**, 3967 (2000).
- ⁸M. Paulsson and S. Stafström, *J. Phys.: Condens. Matter* **12**, 9433 (2000).
- ⁹M. Lögdlund, P. Dannetun, S. Stafström, W. R. Salaneck, M. G. Ramsey, C. W. Spangler, C. Fredriksson, and J.-L. Brédas, *Phys. Rev. Lett.* **70**, 970 (1993).
- ¹⁰V. Enkelmann, in *Electronic Materials: The Oligomeric Approach*, edited by K. Müllen and G. Wegner (VCH-Wiley, Weinheim, 1998).
- ¹¹C. S. Fadley, in *Electron Spectroscopy: Theory, Techniques, and Applications*, edited by C. R. Brundle and A. D. Baker (Academic, London, 1978).
- ¹²H. Tokutaka, N. Ishihara, K. Nishimori, S. Kishida, and K. Isomoto, *Surf. Interface Anal.* **18**, 697 (1992).
- ¹³C. D. Wagner, W. M. Riggs, L. E. Davis, J. F. Moulder, and G. E. Muilenberg, *Handbook of X-ray Photoelectron Spectroscopy* (Perkin-Elmers Corporation, Eden Prairie, MN, 1978).
- ¹⁴D. M. Poirier, D. W. Owens, and J. H. Weaver, *Phys. Rev. B* **51**, 1830 (1995).
- ¹⁵M. J. S. Dewar, E. G. Zoebisch, E. F. Healy, and J. P. Stewart, *J. Am. Chem. Soc.* **107**, 3902 (1985).
- ¹⁶J. L. Brédas, R. R. Chance, R. Silbey, G. Nicolas, and P. Durand, *J. Chem. Phys.* **75**, 255 (1981).
- ¹⁷J. M. André, J. Delhalle, and J. L. Brédas, *Quantum Chemistry Aided Design of Organic Polymers* (World Scientific, Singapore, 1991).
- ¹⁸W. R. Salaneck, *CRC Crit. Rev. Solid State Mater. Sci.* **12**, 267 (1985).
- ¹⁹M. B. J. Meinders, L. H. Tjeng, and G. A. Sawatzky, *Phys. Rev. Lett.* **73**, 2937 (1994).
- ²⁰O. Gunnarsson, *Phys. Rev. B* **54**, R11026 (1996).
- ²¹A. Crispin, M. Fahlman, X. Crispin *et al.*, (unpublished).
- ²²J.-L. Brédas, B. Thémans, J. G. Fripiat, J. M. André, and R. R. Chance, *Phys. Rev. B* **29**, 6761 (1984).
- ²³J. Schnadt, P. A. Brühwiler, N. Mårtensson, A. Lassesson, F. Rohmund, and E. E. B. Campbell, *Phys. Rev. B* **62**, 4253 (2000).
- ²⁴D. A. Morton-Blake, J. Corish, and F. Bénére, *Theor. Chim. Acta* **68**, 389 (1985).
- ²⁵M. Nakadaira, R. Saito, T. Kimura, G. Dresselhaus, and M. S. Dresselhaus, *J. Mater. Res.* **12**, 1367 (1997).
- ²⁶P. Bennich, C. Puglia, P. A. Brühwiler, A. Nielsson, A. J. Maxwell, A. Sandell, N. Mårtensson, and P. Rudolf, *Phys. Rev. B* **59**, 8292 (1999).
- ²⁷J. E. Fisher and T. E. Thompson, *Phys. Today* **6**, 36 (1978).
- ²⁸R. Friedlein, X. Crispin, M. Pickholz, M. Keil, S. Stafström, and W. R. Salaneck, *Chem. Phys. Lett.* **354**, 391 (2002).